Article

Cell Reports

Mir-17∼92 Governs Motor Neuron Subtype Survival by Mediating Nuclear PTEN

Graphical Abstract

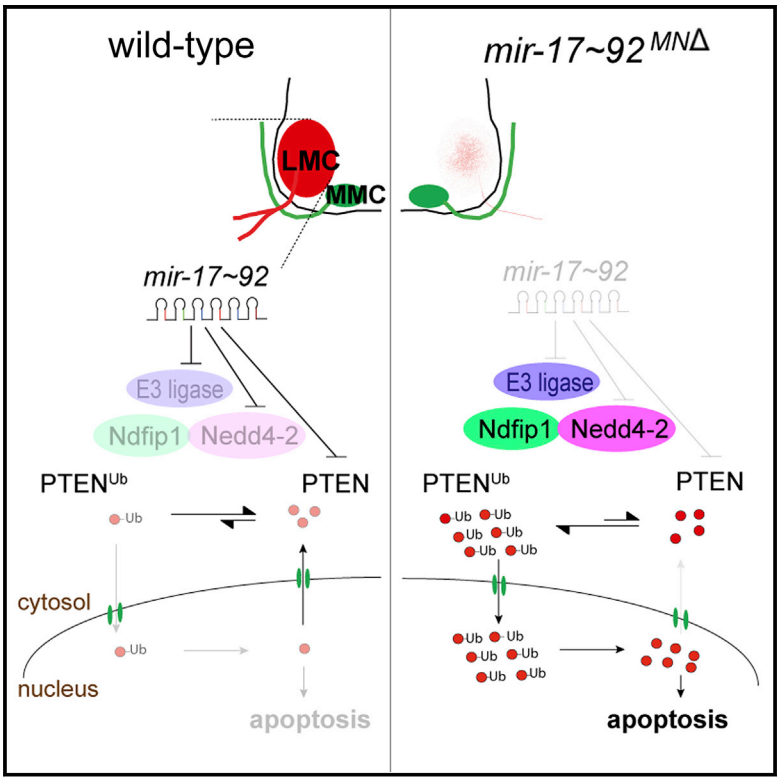

Highlights

- The survival of limb-innervating motor neurons depends upon the *mir-17∼92* cluster
- *mir-17∼92* targets PTEN and E3 ubiquitin ligases to regulate PTEN expression
- miRNA couples post-transcriptional regulation and post-translational modification
- This coupling regulates the subcellular localization of target proteins

Authors

Ying-Tsen Tung, Ya-Lin Lu, ..., Jui-Hung Hung, Jun-An Chen

Correspondence

jachen@imb.sinica.edu.tw

In Brief

Tung et al. show that PTEN is a primary target of *mir-17∼92* and is responsible for limb-innervating motor neuron degeneration. *mir-17∼92* directly targets components of E3 ubiquitin ligases, affecting PTEN subcellular localization through monoubiquitination and providing limb-innervating motor neurons with an intricate defensive mechanism that controls their survival.

Accession Numbers

GSE67795

Tung et al., 2015, Cell Reports *11*, 1305–1318
May 26, 2015 ©2015 The Authors
http://dx.doi.org/10.1016/j.celrep.2015.04.050

Cell Reports
Article

Mir-17∼92 Governs Motor Neuron Subtype Survival by Mediating Nuclear PTEN

Ying-Tsen Tung,[1,7] Ya-Lin Lu,[1,7] Kuan-Chih Peng,[1,2] Ya-Ping Yen,[1,3] Mien Chang,[1] Joye Li,[4] Heekyung Jung,[5] Sebastian Thams,[6] Yuan-Ping Huang,[6] Jui-Hung Hung,[4] and Jun-An Chen[1,*]
[1]Institute of Molecular Biology, Academia Sinica, Taipei 11529, Taiwan
[2]Department of Life Sciences and Institute of Genome Sciences, National Yang-Ming University, Taipei 112, Taiwan
[3]Institute of Biotechnology, College of Bio-Resources and Agriculture, National Taiwan University, Taipei 106, Taiwan
[4]Department of Biological Science and Technology, National Chiao Tung University, Hsinchu 300, Taiwan
[5]Department of Neuroscience and Physiology, Howard Hughes Medical Institute, NYU Neuroscience Institute, New York University School of Medicine, New York, NY 10016, USA
[6]Departments of Pathology and Cell Biology, Neurology, and Neuroscience and Center for Motor Neuron Biology and Disease, Columbia University Medical Center, New York, NY 10032, USA
[7]Co-first author
*Correspondence: jachen@imb.sinica.edu.tw
http://dx.doi.org/10.1016/j.celrep.2015.04.050

SUMMARY

Motor neurons (MNs) are unique because they project their axons outside of the CNS to innervate the peripheral muscles. Limb-innervating lateral motor column MNs (LMC-MNs) travel substantially to innervate distal limb mesenchyme. How LMC-MNs fine-tune the balance between survival and apoptosis while wiring the sensorimotor circuit en route remains unclear. Here, we show that the *mir-17∼92* cluster is enriched in embryonic stem cell (ESC)-derived LMC-MNs and that conditional *mir-17∼92* deletion in MNs results in the death of LMC-MNs in vitro and in vivo. *mir-17∼92* overexpression rescues MNs from apoptosis, which occurs spontaneously during embryonic development. *PTEN* is a primary target of *mir-17∼92* responsible for LMC-MN degeneration. Additionally, *mir-17∼92* directly targets components of E3 ubiquitin ligases, affecting PTEN subcellular localization through monoubiquitination. This miRNA-mediated regulation modulates both target expression and target subcellular localization, providing LMC-MNs with an intricate defensive mechanism that controls their survival.

INTRODUCTION

The coordination of motor behaviors in response to environmental stimuli in animals is mediated by the precise hard-wired connections between motor neurons (MNs) and their peripheral muscle targets. Along the rostrocaudal axis of the neural tube, MNs are spatially divided into columnar subtypes according to the topographical organization of their innervating targets (Dasen, 2009). Medial motor column MNs (MMC-MNs), which span all segmental levels and project to and innervate the epaxial muscles of the dorsal musculature, whereas lateral motor column MNs (LMC-MNs), located at the brachial and lumbar spinal cord levels, innervate limb muscles (Dasen, 2009; Dasen and Jessell, 2009). Specification of the motor columns requires extrinsic signaling pathways that induce sequential Hox transcription-factor-mediated responses (Dalla Torre di Sanguinetto et al., 2008; Dasen and Jessell, 2009). The cross-repressive activities of these Hox genes establish the brachial, thoracic, and lumbar boundaries. Each segment can be further diversified into different motor columns according to the differential expression of the forkhead transcription factor, FoxP1. High FoxP1 expression promotes the induction of LMC-MNs that innervate limb muscles, whereas lower FoxP1 expression levels in the thoracic region generate preganglionic motor column (PGC) neurons that innervate the sympathetic ganglia and hypaxial motor column (HMC) neurons that in turn innervate body wall muscles (Dasen et al., 2008; Rousso et al., 2008).

LMC-MNs are further subdivided into more than 50 pools according to their target muscle connectivity (Dasen et al., 2005). The projecting axon of a motor pool, together with its selective limb mesenchyme, constitutes a functional motor circuit. Emanating from the targeted muscle cells are retrograde-derived neurotrophic factors (NFs; e.g., brain-derived neurotrophic factor [BDNF], glial cell-derived neurotrophic factor [GDNF], neurotrophin-3 [NT3], and ciliary neurotrophic factor [CTNF]) that further support the survival of MNs, as only a subset of MNs receiving NFs will survive, while the rest will undergo apoptosis (Buss et al., 2006b; Dekkers et al., 2013; Hamburger, 1992; Oppenheim, 1991; Raoul et al., 1999). The apoptotic pathways are thought to be dynamically tuned during the relatively long distance, and the axons have to travel, grow, and project to the peripheral areas in the absence of target-derived trophic signals (Burek and Oppenheim, 1996; Oppenheim, 1989, 1991; Raoul et al., 1999). Within the developing CNS, spinal cord MNs are peculiar in that they depend upon target-derived trophic factors for long-term survival. However, it remains unclear whether intrinsic regulation determines this particular neurotrophic dependency of MNs (Raff, 1992).

While Hox proteins and their associated cofactors were identified as the primary determinants of generic and specific MN identity (Dasen, 2009; Dessaud et al., 2008; Philippidou and Dasen, 2013), we and others have previously demonstrated that microRNA (miRNA)-mediated post-transcriptional regulation participates in fine-tuning the programs for MN progenitor specification (Chen et al., 2011), MN differentiation (Chen and Wichterle, 2012), and subtype diversification (Asli and Kessel, 2010; Otaegi et al., 2011). Upon examining mutant embryos with the conditional MN *Dicer* deletion (*Dicer*$^{MN\Delta}$), we have further uncovered a preferential loss of limb- and sympathetic-ganglia-innervating spinal MNs (i.e., LMC and PGC neurons). Additionally, *Dicer*$^{MN\Delta}$ embryos display erosion of motor pool identity. Thus, we suggest that miRNAs, together with the transcription factor network, participate in MN survival and the acquisition of the motor pool signature (Chen and Wichterle, 2012). However, it remains unclear which set of miRNAs and their physiological target genes might be involved in the selective MN degeneration and diversification. Previously, we demonstrated that *mir-17-3p* in the *mir-17∼92* cluster participates in the Olig2/Irx3 transcription factor loop to carve out the p2/MN progenitor (pMN) boundary (Chen et al., 2011). Unexpectedly, we further identified the *mir-17∼92* cluster as the culprit behind the selective degeneration of limb-innervating MNs in the *Dicer*$^{MN\Delta}$ embryos. We found that *mir-17∼92* is highly enriched in LMC-MNs. MNs with the *mir-17∼92* deletion (*mir-17∼92*$^{MN\Delta}$) lead to the selective cell death of LMC-MNs in vitro and in vivo, which partially phenocopies *Dicer*$^{MN\Delta}$ embryos. Furthermore, we identified *PTEN* as a primary target of *mir-17∼92* in MNs, and we found that *mir-17∼92* not only regulates *PTEN* expression but also mediates PTEN ubiquitination levels. We verified a set of E3 ubiquitin ligases (*Nedd4-2*, *Ndfip1*, *Klhdc5*, and *Ube3b/c*) as *mir-17∼92* bona fide targets that are upregulated in the *mir-17∼92* knockout (KO) MNs. An increase in E3 ligases leads to PTEN monoubiquitination, thereby promoting PTEN nuclear import (Howitt et al., 2012; Song et al., 2011; Trotman et al., 2007). Moreover, overexpression of *mir-17∼92* in MNs in the embryo rescues MNs from apoptosis during embryo development by attenuating PTEN expression and nuclear import. Our findings provide evidence of an intrinsic circuit that controls apoptosis in specific neuronal types in the CNS during neural development. Furthermore, our results suggest a sophisticated model that regulates target subcellular localization by coupling the post-transcriptional regulation and post-translational modification mediated by miRNAs.

RESULTS

Mir-17∼92 Is Critical to the Survival of Limb-Innervating MNs

To determine whether the miRNA biogenesis pathway contributes to MN differentiation and maturation in mouse embryos, we previously demonstrated that conditional MN-*Dicer* deletion (*Dicer*$^{MN\Delta}$) results in the loss of limb- and sympathetic-ganglia-innervating spinal MNs accompanied by an increase in apoptosis in the ventral horn (Chen and Wichterle, 2012). However, the causal miRNAs and their targets that underlie specific MN subtype degeneration are still unknown. As indicated by previous reports, *mir-17∼92* can promote tumor formation by inhibiting apoptosis (Mu et al., 2009; Olive et al., 2009, 2010); therefore, we hypothesized that *mir-17∼92* might function as a double-edged sword that initially controls MN generation by carving out the pMN boundary (Chen et al., 2011) and then, at a later stage, governs MN degeneration by balancing apoptosis in the developing spinal cord.

To verify our hypothesis, we analyzed if the absence of the *mir-17∼92* cluster would lead to preferential apoptosis in the MN subtype (i.e., LMC and PGC neurons). We first examined the distribution of cells undergoing apoptosis in the embryonic spinal cord at the brachial (∼C5–C8), thoracic (∼T1–T13), and lumbar (L1∼L6) segments from approximately embryonic day 11.5 (E11.5) to E13.5 in control and *mir-17∼92*-KO embryos (Figure S1A). Wild-type (WT) and KO embryos were indistinguishable at E11.5 in terms of the number of active apoptotic cells (revealed by active cleaved caspase-3 immunostaining, cCasp3^{on}). Interestingly, at E13.5, although the increase in cCasp3^{on} cells was not evident in the thoracic region of the spinal cord, there was a robust spread of cCasp3^{on} cells in the ventral horn of the brachial and lumbar spinal segments (Figure S1B). Specific staining for cCasp3 in the ventral horns of the brachial/lumbar segments suggested that certain MN subtypes in the ventral spinal cord might be affected. We therefore performed a series of immunostaining experiments to reveal which neuronal populations were undergoing apoptosis in the *mir-17∼92*-KO embryos (Figure 1). Consistent with the cCasp3^{on} areas in the brachial and lumbar spinal cords, we detected a significant decrease (∼55%) in the number of FoxP1^{on} and Raldh2^{on} limb-innervating LMC neurons, whereas other MN subtypes (for instance, MMC-MNs labeled by Lhx3^{on} and HMC-MNs labeled by Isl1^{on} and Lhx3^{off}) did not appear to diminish in number (Figures 1A–1F, quantification in Figure 1G). Furthermore, the axons of lumbar MNs expressing *Hb9::GFP* projected ventrolaterally toward the limb bud and dorsolaterally to the axial muscles in the WT embryos. However, axons in the *mir-17∼92*-KO embryos projected to limb muscles with thinner bundles that exhibited arborization defects (Figures 1H–1M, summary in Figure 1N). Collectively, these results indicate that the loss of the *mir-17∼92* cluster results in a striking degeneration of specific MN subtypes, particularly the limb-innervating LMC-MNs.

mir-17∼92 Expression Is Specifically Enriched in LMC-MNs In Vitro and In Vivo

Preferential LMC-MN degeneration in the *mir-17∼92* mutant embryos prompted us to examine whether this phenotype is caused by differential expression of the *mir-17∼92* cluster in the MN subtypes. In situ hybridization of mouse E12.5 spinal cord revealed that *mir-17-5p* (one of the *mir-17∼92* cluster members) was enriched in the region of postmitotic MNs (Figures 2A–2G). Fluorescent miRNA in situ hybridization, together with immunohistochemistry on the same section of mouse E10.5 and E12.5 spinal cord, further showed that both *mir-17-5p* and *mir-17-3p* had enriched expressions in the LMC (FoxP1^{on}, Isl1/2^{on}) region but reduced expressions in the MMC domain (FoxP1^{off}, Hb9^{on}) (Figure 2C, 2F, and S2).

Although in situ hybridization provided the spatial distribution of *mir-17∼92* expression in the spinal cord, it could not indicate

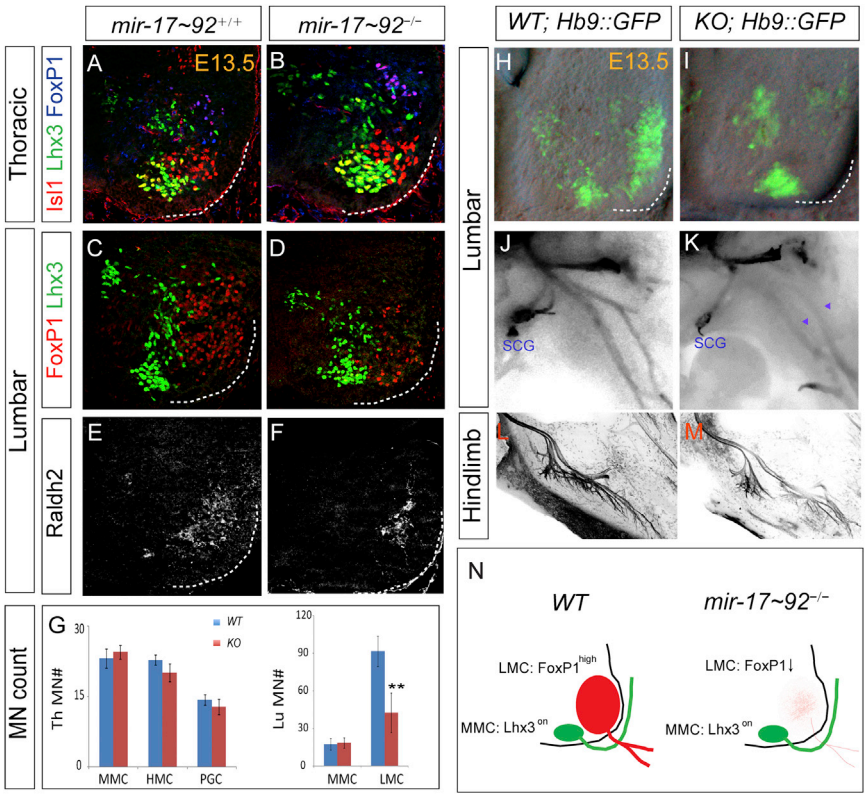

Figure 1. *mir-17~92* Is Critical for the Survival of Limb-Innervating MNs

(A and B) Immunostaining reveals comparable numbers of PGC (FoxP1^{low}), MMC (Lhx3^{on}), and HMC (Lhx3^{off}, IsL1^{on}) MNs in the thoracic spinal cord sections of E13.5 *mir-17~92* mutant embryos.

(C–F) Immunostaining at lumbar spinal cord sections points to a decrease in LMC-MNs (Raldh2^{on}, FoxP1^{high}) in E13.5 *mir-17~92* mutant embryos, whereas MMC-MNs (Lhx3^{on}, FoxP1^{off}) are not affected.

(G) Quantification of PGC (FoxP1^{low}), MMC (Lhx3^{on}), and HMC (Lhx3^{off}, IsL1^{on}) MNs in the thoracic spinal cord, and LMC (Raldh2^{on}, FoxP1^{high}) and MMC (Lhx3^{on}, FoxP1^{off}) MNs in the lumbar spinal cord (number of positive cells per 20 μm spinal cord ventral half section) in control and *mir-17~92* mutant embryos (mean ± SD, n = 8 embryos). Only the decrease in LMC-MNs is significant (**p < 0.01).

(H–M) Axonal projections and innervations at lumbar levels in the wild-type (WT) and *mir-17~92* mutants (KO) revealed by *Hb9::GFP*. In KO embryos, the decrease in thickness of the motor nerve branch projecting to the limb reflects the depletion of FoxP1^{high} LMC-MNs (arrowhead), and the arborization of motor axons is drastically reduced. Projections to axial muscles are preserved (250 μm spinal cord ventral half section).

(N) Schematic indicating how *mir-17~92* controls the survival of LMC columns and axon projection.

the differential expression in MN subtypes quantitatively. To circumvent the limitation of obtaining homogenous LMC-MNs in vivo, we derived an embryonic stem cell (ESC) harboring a GFP reporter under the control of a bacterial artificial chromosome (BAC) containing ~195 kb of the 5′ *FoxP1* sequence (Jung et al., 2014). Under caudalized differentiation conditions (Mazzoni et al., 2013), ESCs acquired the brachial identity (Hoxc6^{on}, data not shown) with ~5%–10% GFP^{on} cells (Figures 2H and 2I). The majority of the GFP^{on} cells were FoxP1^{on}, Isl1/2^{on}, Raldh2^{on}, and Lhx3^{off} cells (Figures 2J–2M). Quantitative real-time PCR further confirmed a ~10-fold enrichment in the expression of the specific LMC marker gene, *Raldh2*, in fluorescence-activated cell sorting (FACS)-arranged GFP^{on} cells when compared to control GFP^{off} cells and generic MNs derived from *Hb9::GFP* ESCs (Figures 2N and S2C). From the same set of *FoxP1::GFP*^{on} cells, the expression of most of the *mir-17~92* cluster members displayed a ~5- to 10-fold enrichment compared to control GFP^{off} and generic *Hb9::GFP*^{on} MNs. Taking all of these analyses together, we concluded that the expression of the *mir-17~92* cluster is more enriched in limb-innervating MNs than in other MN subtypes.

mir-17~92 Has Cell-Autonomous Functions in LMC-MNs

As *mir-17~92* is also expressed in Isl1/2^{on} dorsal root ganglion (DRG) neurons and the adjacent somite (Figure S2B), we sought to determine whether the loss of selective LMC-MNs is due to intrinsic cell-autonomous defects in spinal MNs or to extrinsic signals from neighboring cells.

To dissect the cell-autonomy effect in a "salt and pepper" manner, we generated embryoid bodies (EBs) composed of a 50:50 mixture of control *Hb9::RFP* ESCs with either WT or null *mir-17~92 Hb9::GFP* ESCs (Figures 3A–3D). The cells aggregated into mixed EBs, and the ratios of WT GFP^{on}/control RFP^{on} MNs and null GFP^{on}/control RFP^{on} MNs were determined following MN apoptosis on day 7. The quantifications indicated that apoptosis caused by *mir-17~92* deletion was primarily due to cell-autonomous defects in MNs, as the number of control RFP^{on} motor neurons was unchanged whereas the number of GFP^{on} null MNs was significantly reduced.

To complement the in vitro studies, we performed MN-specific deletion of *mir-17~92 in vivo* (*mir-17~92*$^{MN\Delta}$: *Olig2*$^{Cre/+}$; *mir-17~92* ^{floxed}). The *mir-17~92*$^{MN\Delta}$ embryos were not born according to the Mendelian ratio, indicating that some embryos die prenatally or perinatally (Table S1). Among the surviving embryos, ~60% of the mice manifested gross locomotive deficits postnatally (postnatal day 30 [P30]; Movie S1).

Consistent with the *mir-17~92*-null embryo analysis, we detected a significant decrease in the number of FoxP1^{on} limb-innervating LMC neurons (Figures 3E and 3F), with a concomitant increase in apoptotic cells (cCasp3^{on} and Bim^{on}) (Figures 3I–3L), whereas other MN subtypes (MMC- and HMC-MNs) appeared normal in the *mir-17~92*$^{MN\Delta}$ embryos (Figures 3G and 3H, quantification in Figure 3O). As previous studies reported that the *mir-17~92* cluster plays dual roles by either promoting cell proliferation or inhibiting the apoptotic pathway in tumors (Mu et al., 2009; Olive et al., 2009; Olive et al., 2013), we further examined whether the apoptosis of MN cells in the absence of

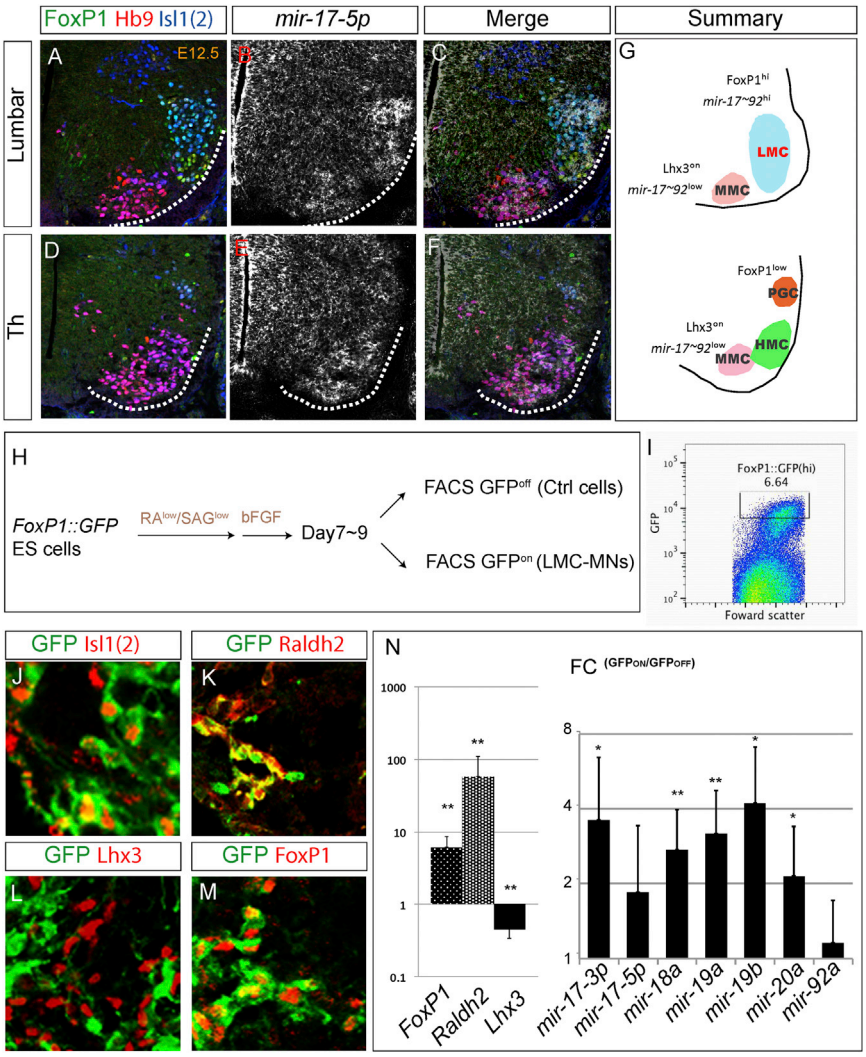

Figure 2. Specific Enrichment of *mir-17∼92* in LMC-MNs In Vitro and In Vivo

(A–F) Expression of *mir-17-5p* examined by fluorescence in situ hybridization together with immunostaining on E12.5 spinal cord sections.

(G) Schematic describing the expression pattern of *mir-17∼92* together with other transcription factors in the spinal cord.

(H) Schematic illustration of ESC-derived LMC-MNs. *FoxP1::GFP* ESC lines were differentiated with caudalized medium on day 2. GFP^{on} LMC-MNs were sorted by FACS, whereas GFP^{off} cells were preserved as a control.

(I) FACS analysis (density plots) of *FoxP1::GFP* ESCs differentiated under caudalized conditions in (H). Rectangle indicates the gate used for sorting GFP^{on} LMC-MNs.

(J–M) Immunostaining of EBs on day 8 reveals that GFP^{on} cells display the molecular characteristics of LMC-MNs (IsL1/2^{on}, Raldh2^{on}, FoxP1^{on}, Lhx3^{off}).

(N) Verification of immunostaining by quantitative real-time PCR from independent differentiation experiments. *FoxP1* and *Raldh2* show a 10- to 60-fold increase, while the *mir-17∼92* cluster also displays an ∼2- to 4-fold enrichment in *FoxP1::GFP*^{on} cells when compared to GFP^{off} cells. FC, fold change. Data represent at least three independent experiments (n > 3) performed in duplicate. Error bars indicate the SD (*p < 0.05, **p < 0.01).

mir-17∼92 is a consequence of overproliferation at the progenitor stage. *mir-17∼92*-KO embryos at E11.5 displayed comparable numbers of proliferating cells (phospho-histone H3, $pH3^{on}$) to WT embryos (Figure S3A), suggesting that *mir-17∼92* controls the survival of postmitotic MNs by inhibiting apoptosis rather than by promoting cell proliferation.

Given that a small portion of LMC-MNs were preserved in the *mir-17∼92*$^{MN\Delta}$ embryos, we wanted to determine whether the remaining MNs acquired the proper subtype identities. We examined the expression of motor pool subtype-specific markers in the mutant spinal cord. Despite the severe reduction of LMC-MNs, several sets of lumbar motor pool genes were preserved (Nkx6.1^{on}, Figures 3M and 3N; Pea3^{on}, data not shown) in the remaining LMC-MNs. The selective loss of FoxP1^{on} LMC-MNs was not caused by the impairment of upstream Hox proteins, as the expression levels of Hoxc6 and Hoxc9 were unaffected prior to MN apoptosis at E11.5 in the *mir-17∼92*-null embryos (Figure S3B).

Although the *Olig2*$^{Cre/+}$ driver we used also deleted the expression of *mir-17∼92* in oligodendrocyte precursors (Chen and Wichterle, 2012), immunostaining of E14.5 spinal cords of *mir-17∼92*$^{MN\Delta}$ embryos for oligodendroglial and astrocytic markers revealed a comparable number of oligodendroglial progenitor cells expressing Olig2 and Sox9 (Figure S3C). These results further supported our assumption that the loss of the *mir-17∼92* cluster results in cell-autonomous MN subtype-specific degeneration.

mir-17∼92 Regulates the Survival of LMC-MNs prior to Neurotrophic Support

In the developing spinal cord, only half of the nascent MNs survive while the rest undergo apoptosis. It has long been hypothesized that the apoptosis of MNs relies on the NFs from innervating targets (Burek and Oppenheim, 1996; Buss et al., 2006b; Oppenheim, 1991). A previous study also revealed that the long-term survival of dissociated ESC-derived MNs is dependent upon NFs (Wichterle et al., 2002), which raises the possibility that the presence of NFs controls the apoptosis of MNs. However, the selective apoptosis of LMC-MNs in *mir-17∼92*$^{MN\Delta}$ embryos is most dramatic when MNs are about to contact their targets, suggesting it is unlikely that the absence of NFs is the primary factor initiating apoptosis during this time.

To investigate this point further, we differentiated WT and *mir-17∼92*$^{-/-}$ ESCs into MNs and profiled apoptosis ($AnnexinV^{on}$) in the EBs either with or without NF cocktails before dissociation

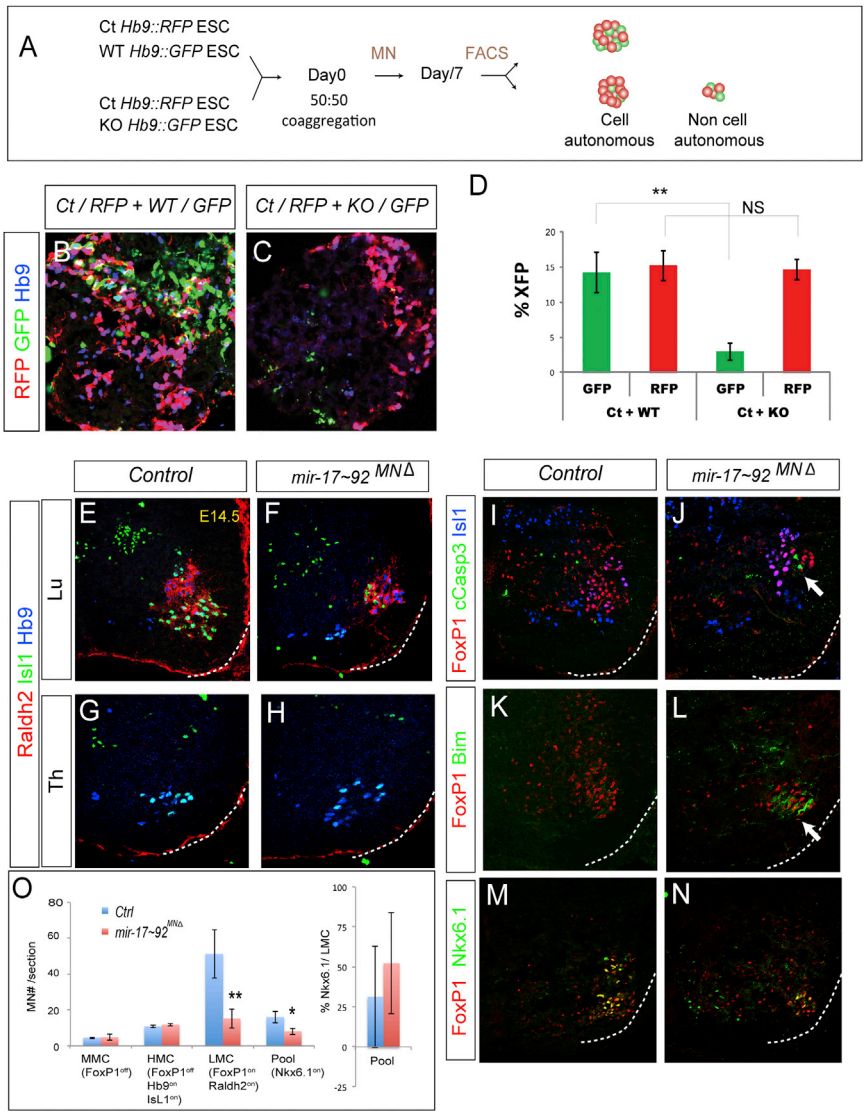

Figure 3. Cell-Autonomy Effect of *mir-17~92* in MNs In Vitro and In Vivo

(A) Schematic illustrating the effects of cell autonomy by the "salt and pepper" approach. Control *Hb9::RFP* together with *mir-17~92* WT or KO *Hb9::GFP* ESCs are mixed in 50:50 ratios and differentiated into MNs. The percentages of RFP^{on} and GFP^{on} cells were measured by FACSCalibur. Non-cell-autonomous effects of *mir-17~92* KO can be deduced by the subsequent quantification of the percentage of control $Hb9::RFP^{on}$ cells.

(B and C) Immunostaining of day 7 EBs reveals that the control RFP^{on} cells are not affected by either mixing with WT or *mir-17~92*-KO MNs.

(D) Quantification of the florescence percentage (%XFP) in total EBs after dissociation on day 7 by FACSCalibur (n = 3 independent experiments, mean ± SD, $^{**}p < 0.01$).

(E–H) Immunostaining of lumbar spinal cord sections indicates a decrease in LMC-MNs ($Raldh2^{on}$, $Isl1^{on}$) in E14.5 $mir\text{-}17\sim92^{MN\Delta}$ embryos, yet MMC ($FoxP1^{off}$) and HMC ($Isl1^{on}$, $FoxP1^{off}$) MNs in the thoracic segment were not affected.

(I–N) The decrease in LMC-MNs in the lumbar spinal cord is accompanied by an increase in apoptotic markers ($cCasp3^{on}$ and Bim^{on}) (arrowhead). The spared LMC-MNs still express motor pool markers, such as $Nkx6.1^{on}$.

(O) Quantification of MMC ($FoxP1^{off}$, $Lhx3^{on}$) and HMC ($Isl1/Hb9^{on}$, $FoxP1^{off}$) MNs in the thoracic spinal cord and LMC ($Raldh2^{on}$, $FoxP1^{on}$) and motor pool ($Nkx6.1^{on}$) MNs in the lumbar spinal cord (number of positive cells per 20 μm of spinal cord in the ventral half section) in control and $mir\text{-}17\sim92^{MN\Delta}$ embryos. Although the reduction of LMC-MNs was significant ($^{**}p < 0.01$), the percentage of the Nkx6.1^{on} pool in $FoxP1^{on}$ neurons was not affected in the $mir\text{-}17\sim92^{MN\Delta}$ embryos (mean ± SD, n = 8 embryos).

(Figure S4). As expected, $mir\text{-}17\sim92^{-/-}$ MNs exhibited more prominent apoptosis at the nascent postmitotic stage (days ~6–7) when compared to WT-MNs. However, NFs did not rescue the apoptotic phenotype in the WT or $mir\text{-}17\sim92^{-/-}$ MNs (Figures S4C and S4D), suggesting that the MN death that naturally occurs at an early stage is independent of target-derived NFs.

mir-17~92 Targets *PTEN* and Regulates Its Subcellular Localization

The prominent intrinsic LMC-MN apoptosis caused by the deletion of *mir-17~92* prompted us to seek the responsible targets. To identify the targets of the *mir-17~92* cluster that are involved in MN degeneration, primary MNs in the spinal cord from WT and $mir\text{-}17\sim92^{-/-}$; *Hb9::GFP* embryos at E12.5 were isolated by FACS (Figure 4A). Subsequently, WT and $mir\text{-}17\sim92^{-/-}$ MN (GFP^{on}) and non-MN (GFP^{off}) transcriptomes were analyzed by microarrays. The sets of genes that were upregulated in null MNs only (fold change ≥ 1.5, n = 2) compared to WT controls were filtered with in-silico-predicted targets (Grimson et al., 2007). Gene ontology analysis using the Database for Annotation, Visualization, and Integrated Discovery (DAVID) (Huang et al., 2009) on only those genes that were upregulated in null MNs indicated the involvement of these genes in the regulation of apoptosis, protein ubiquitination, and protein localization (Figure S5A; Table S2). With increasing stringency, we identified 15 candidate targets of *mir-17~92* that were predicted to participate in the apoptotic pathway (Figures 4A and S5B). Among the top candidates, we first verified that the expression of *PTEN* was significantly upregulated in the MNs from *mir-17~92*-KO embryos by quantitative real-time PCR (Figure 4B), as *PTEN* was previously shown to be a direct target of *mir-17~92* in tumor cells and cortical neurons (Bian et al., 2013; Mu et al., 2009; Olive et al., 2010; Xiao et al., 2008). In the developing spinal cord, the expression of PTEN was enriched in postmitotic neurons at E11.5 (Figure S5C). However, by E12.5, PTEN expression declined and was distributed mainly in the cytoplasmic regions of MNs in the WT embryos, whereas PTEN remained strongly expressed and was translocated into the nuclei in the *mir-17~92*-KO embryos

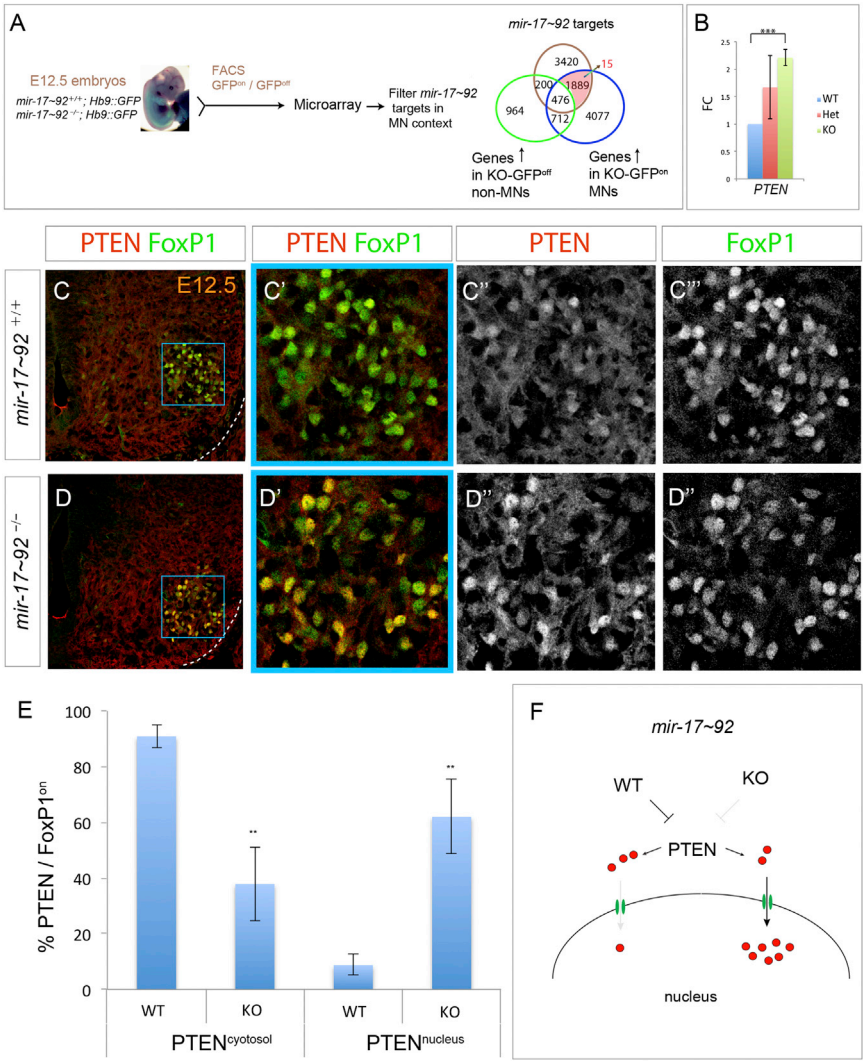

Figure 4. Accumulation of Nuclear PTEN in the *mir-17~92* Mutant Embryos

(A) Strategy to identify *mir-17~92* targets in MNs. The Venn diagram illustrates a set of target candidate genes from the intersection of upregulated genes found only in the *mir-17~92*-KO MNs that were predicted to be direct targets of *mir-17~92* by TargetScan. Genes predicted to be targeted by more than one member of the *mir-17~92* cluster allowed us to narrow down the targets to 15 genes, including *PTEN*.

(B) Verification of microarray data by quantitative real-time PCR in the WT, heterozygous (Het), and *mir-17~92*-KO FACS sorted MNs of E12.5 embryos. Data represent three embryos (n = 3) performed in duplicate for each embryo. FC, fold change. Error bars indicate the SD. ***$p < 0.001$.

(C and D) Immunostaining of lumbar spinal cord sections reveals an accumulation of nuclear PTEN in FoxP1^{on} limb-innervating MNs in E12.5 *mir-17~92*-KO embryos (high power magnification in D′), whereas the expression of PTEN declines and remains mostly in the cytosol of WT embryos (C′).

(E and F) Quantification of PTEN expression upon FoxP1^{on} MNs from Figure 5C and 5D indicates a ~5-fold increase of PTEN^{nulceus} protein expression in the *mir-17~92*-KO embryos when compared to the WT.

(Figures 4C and 4D, with high magnification in Figures 4C′ and 4D′). To determine the ratio of PTEN$^{nucleus/cytosol}$ in the absence of the *mir-17~92* cluster, we quantified PTEN expression and its subcellular localization in FoxP1^{on} MNs and revealed a significant increase in PTEN^{nucleus} of LMC-MNs in KO embryos (n = 5, Figure 4E). Collectively, we suggest that the upregulated PTEN produced by *mir-17~92* deletion is mostly translocated into the nuclei of LMC-MNs (Figure 4F).

mir-17~92 Attenuates Nuclear PTEN Accumulation by Targeting E3 Ubiquitin Ligases

Next, we addressed the purpose of PTEN being imported into the nucleus of LMC-MNs in the *mir-17~92*-KO embryos. Several reports have proposed that PTEN nuclear translocation is stimulated by the monoubiquitination of PTEN by E3 ubiquitin ligases, such as the Nedd4/Ndfip1 complex (Howitt et al., 2012; Mund and Pelham, 2010; Trotman et al., 2007; Van Themsche et al., 2009) (summary in Figure 5A). Coincidentally, the expression levels of several known E3 ubiquitin ligases for PTEN, such as Nedd4-2/Ndfip1 and other E3 ligase-associated proteins (Klhdc5 and Ube3b/c), were also upregulated in the MNs of *mir-17~92*-KO embryos (Figures 5B and S5D). As the number of LMC-MNs is limited in vivo, we sought to use an in vitro ESC differentiation system to perform the biochemical analysis. We derived a conditional *CAGGS::CreER*, *mir-17~92^{floxed}* ESC and deleted the *mir-17~92* locus after pMN was established during MN differentiation (Figure S6A). Compared to control (*mir-17~92 ^{floxed}*) ESC-derived EBs, postmitotic MNs (Isl1^{on}, Hb9^{on}) were reduced by ~50% in the *mir-17~92*-KO EBs on differentiation day 7 while remaining unaffected at the progenitor stage (days ~4–5) (Figures S6B and S6C). Furthermore, expressions of the PTEN/Ndfip1/Nedd4-2 proteins were all significantly upregulated, with prominent nuclear PTEN accumulation in the *mir-17~92*-KO ESC-derived MNs, indicating that the in vitro ESC differentiation system recapitulated the phenotype in vivo (Figures 5B and S6D).

To determine whether PTEN and the E3 ubiquitin ligase-associated proteins were direct targets of *mir-17~92*, we constructed luciferase reporter plasmids containing the 3′ UTR of the candidate genes harboring the predicted *mir-17~92* target sites (Figures 5C and S7A). The luciferase constructs (including Olig2 3′ UTR as a known target control and Hoxc6 3′ UTR, which does not contain predicted *mir-17~92* targets, as a negative control) were transfected into *mir-17~92*-KO ESCs. Compared to the WT ESCs, the transfected cells exhibited an ~30%–100% increase in luciferase activity (Figures 5C and S7B). Moreover, luciferase assays

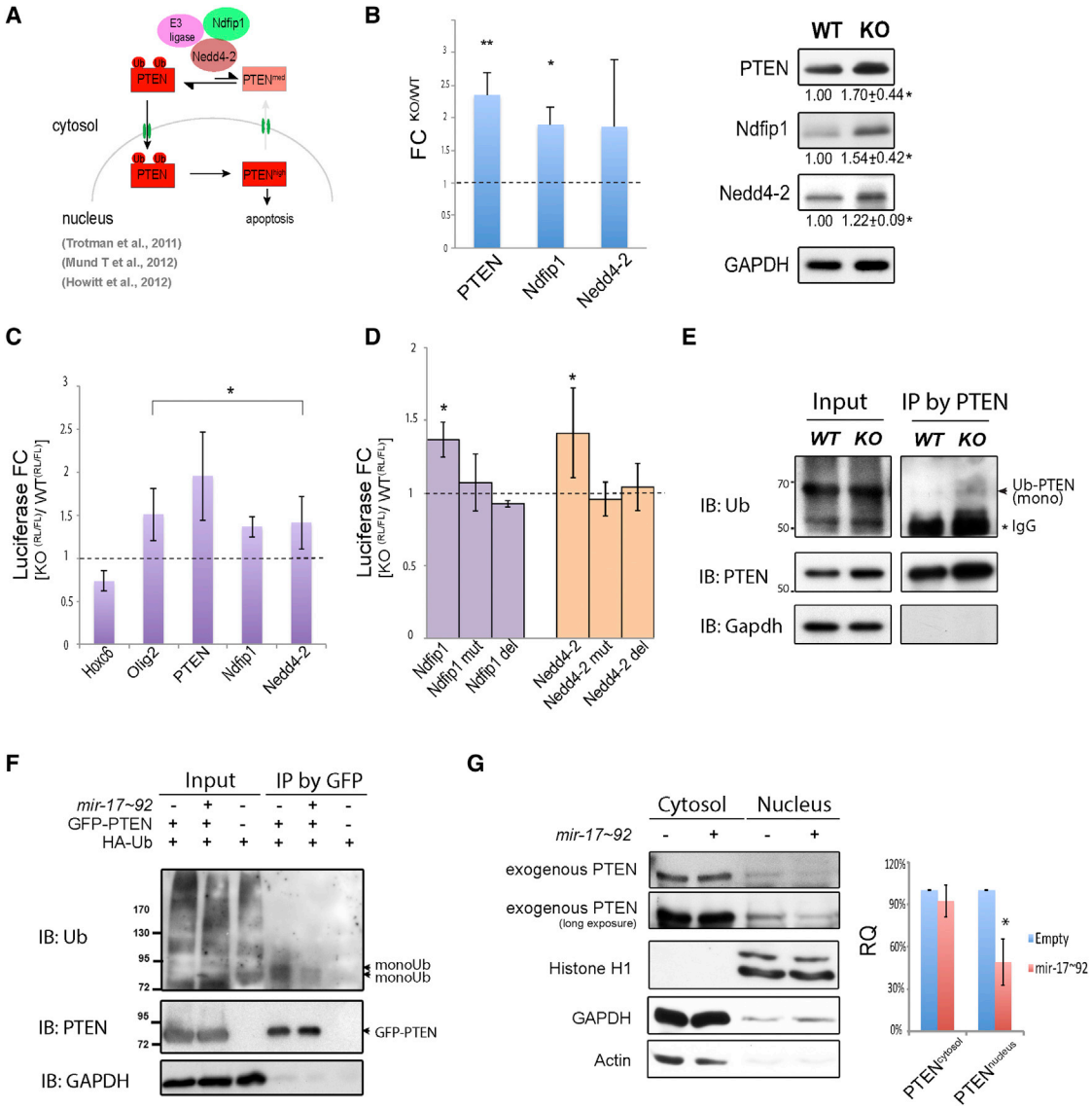

Figure 5. *mir-17∼92* Controls PTEN Subcellular Localization by Directly Targeting E3 Ubiquitin Ligases

(A) Illustration of PTEN monoubiquitination and nuclear transport.

(B) Quantitative real-time PCR assays (left panel) and western blotting (right panel) confirmed that the expression of PTEN and its E3 ubiquitin ligases are upregulated in the *mir-17∼92*-KO ESC-derived MNs compared to in the WT under caudalized conditions. Data represent three independent differentiation experiments (n = 3) performed in duplicate. Error bars indicate the SD. *$p < 0.05$, **$p < 0.01$.

(C and D) Luciferase reporters were constructed with a control in which the potential target sites of *mir-17∼92* were mutated or deleted, and were performed in duplicate ($n \geq 3$ independent experiments, mean ± SD, *$p < 0.05$).

(E) Endogenous PTEN monoubiquitin adducts increased in the *mir-17∼92*$^{-/-}$-derived EBs. Molecular weights are shown in kDa.

(F) Immunoprecipitation of GFP-PTEN after HA-ubiquitin co-expression in 293T cells confirmed the reduction of monoubiquitin adducts when overexpressing *mir-17∼92*. Molecular weights are shown in kDa.

(G) Subcellular fractionation assays indicated an ∼50% increase in exogenous PTEN^{nuclues} (without 3′ UTR) when *mir-17∼92* was overexpressed in 293T cells, whereas exogenous PTEN^{cytosol} remained unaffected (n = 3 independent experiments, mean ± SD, *$p < 0.05$).

confirmed that the mutated putative binding sites or truncated 3′ UTR reporters of the Ndfip1 and Nedd4-2 constructs were completely insensitive to *mir-17∼92*-mediated silencing (Figure 5D). Together with data from qPCR, western blotting, and luciferase assays, we concluded that *Ndfip1*, *Nedd4-2*, and *PTEN* are bona fide *mir-17∼92*-mediated targets in MNs (Figure S7C).

Subsequently, we investigated to what extent PTEN monoubiquitination is regulated by *mir-17∼92*. As shown in Figure 5E, the level of PTEN^{monoUb} was increased in the *mir-17∼92*-KO ESC-derived MNs upon caudalized conditions on differentiation day 6. Consistent with this, the levels of exogenous PTEN^{monoUb} (without 3′ UTR) were reduced upon *mir-17∼92*

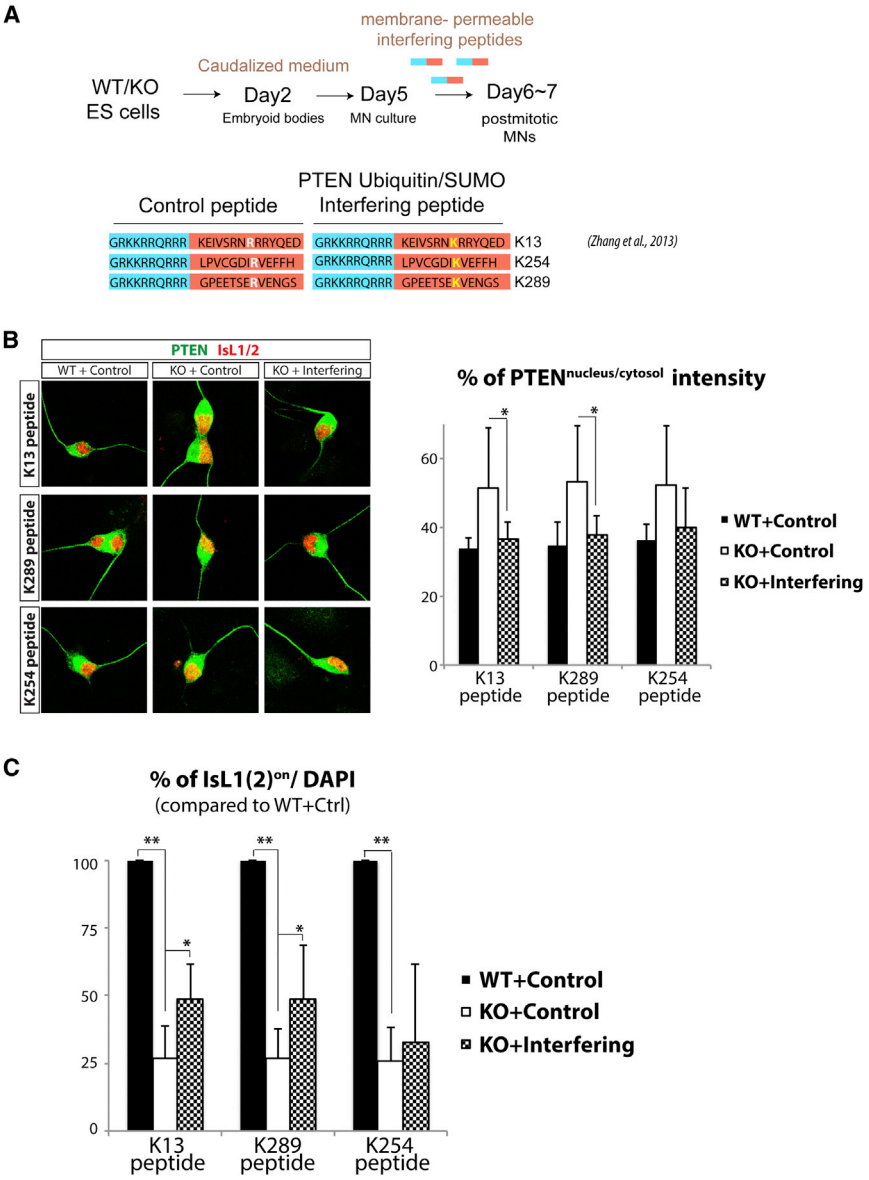

Figure 6. PTEN Ubiquitination-Interfering Peptides Attenuate Nuclear PTEN Levels to Rescue MNs

(A) Schematic illustration of peptide treatment. WT and *mir-17∼92*$^{-/-}$ ESC lines were differentiated with caudalized medium on day 2 and were dissociated on day 5, followed by cell-penetrating peptide treatment (15 μM) for 24–48 hr. Blue bars denote Tat-cell-penetrating peptides, while orange bars denote control or interfering peptides of PTEN K13, K254, or K289 Ub/SUMO sites (see the Supplemental Experimental Procedures for details).

(B) The increased PTEN$^{nucleus/cytosol}$ ratio in control-peptide-treated-*mir-17∼92*-KO MNs (compared to WT MNs) is significantly attenuated by either K13- or K289-interfering peptides.

(C) MN survival (determined by IsL1(2)^{on}/total DAPI^{on} nuclei) in *mir-17∼92*-KO MNs is significantly rescued by either K13- or K289-interfering peptides but is only slightly rescued by the K254-interfering peptide. Quantitative data represent at least three independent experiments (mean ± SD; *p < 0.05, **p < 0.01).

overexpression in 293T cells (Figures 5F and S7D). Therefore, our data demonstrated that *mir-17∼92* targets PTEN and E3 ubiquitin ligases directly, thereby regulating the level of PTEN monoubiquitination.

Finally, to establish whether nuclear PTEN accumulation in the *mir-17∼92*-KO embryos was caused by an increase in the total PTEN protein level or by upregulation of E3 ubiquitin ligase activity resulting in enhanced PTEN^{monoUb} nuclear import, we co-transfected Flag- and hemagglutinin (HA)-tagged PTEN (without 3′ UTR), an exogenous ubiquitin, together with *mir-17∼92* into 293T cells. Subcellular fractionation revealed a significant reduction (∼50%) in the nuclear PTEN protein level, whereas the cytoplasmic levels appeared unchanged (Figure 5G). This result implies that the nuclear PTEN accumulation mediated by *mir-17∼92* is attributed to active nuclear import mechanisms instead of passive diffusion of upregulated PTEN proteins.

mir-17∼92 Mediates PTEN Nuclear Import Directly via Monoubiquitination

In addition to monoubiquitination at the K13 and K289 residues, nuclear translocation of PTEN has also been proposed to be regulated via other post-translational modification mechanisms, such as by sumoylation at the K254 residue (Bassi et al., 2013). To disentangle which modification of PTEN accounts for PTEN accumulation in the *mir-17∼92*-KO MNs, we designed three cell-membrane-permeable interfering peptides that flank the K13/K254/K289 residues of PTEN and performed rescue experiments in control and *mir-17∼92*-KO MN cultures. Consistent with our observations, the *mir-17∼92*-mediated PTEN nuclear translocation was attenuated and MN apoptosis was significantly rescued by the K13/K289-interfering peptides, yet only slightly affected by the K254 peptide, indicating that nuclear PTEN accumulation in *mir-17∼92*-KO LMC-MNs was predominantly caused by PTEN monoubiquitination (Figures 6B and 6C). Collectively, our results indicate that *mir-17∼92* governs MN survival by mediating PTEN nuclear accumulation through monoubiquitination. Blocking ubiquitination of PTEN attenuates its nuclear translocation, thereby preventing apoptosis of MNs in the absence of *mir-17∼92*.

Overexpression of *mir-17∼92* Prevents Naturally Occurring Cell Death

We reasoned that if *mir-17∼92* regulates MN survival intrinsically by mediating PTEN subcellular localization, then the overexpression of *mir-17∼92* in pMNs should surpass the naturally

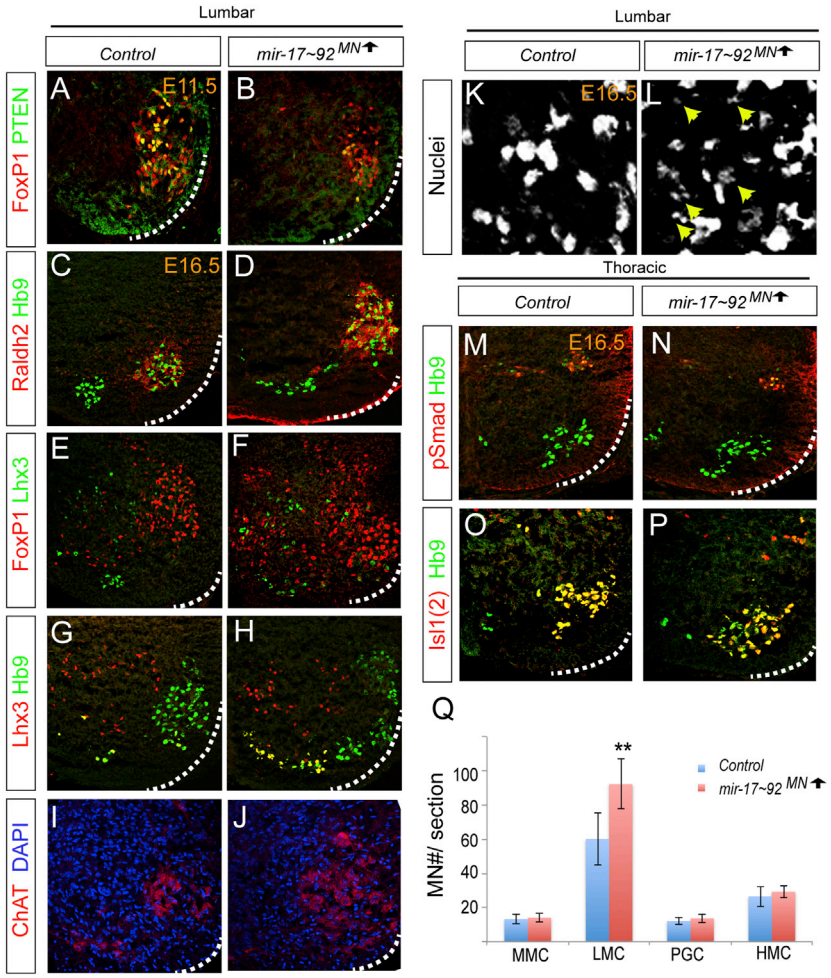

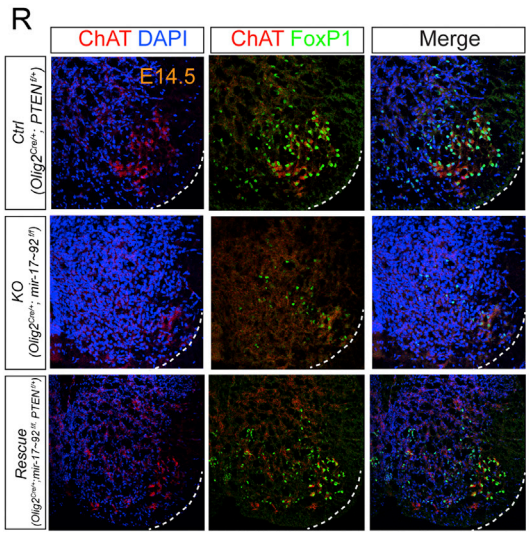

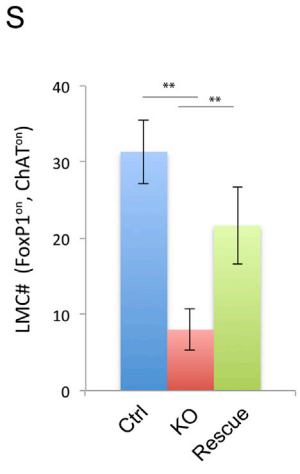

Figure 7. Overexpression of *mir-17∼92* Rescues Intrinsic MN Apoptosis, and Knockdown of PTEN Rescues LMC-MN Degeneration in *mir-17∼92*$^{MN\Delta}$

(A and B) PTEN expression and nuclear import is attenuated in the E11.5∼12.5 *mir-17∼92*$^{MN\uparrow}$ (*Olig2*$^{Cre/+}$; *ROSA26* $^{CAG\text{-}MIR17\text{-}92,\text{-}EGFP}$) lumbar spinal cords.

(C–L) Immunostaining of lumbar spinal cord sections indicates a drastic increase in LMC-MNs (Raldh2^{on}, FoxP1^{on}) in E16.5 *mir-17∼92* $^{MN\uparrow}$ embryos, whereas MMC-MNs (Lhx3^{on}, FoxP1^{off}) increase slightly, but not significantly. The increase in MNs in *mir-17∼92* $^{MN\uparrow}$ embryos exhibits a small nuclei phenotype (arrowhead in L) with enhanced ChAT^{on} expression.

(M–P) Immunostaining in the thoracic spinal cord sections demonstrates comparable numbers of PGC (pSmad^{on}) and HMC (Lhx3^{off}, Isl1^{on}) MNs in E16.5 *mir-17∼92* $^{MN\uparrow}$ embryos. (Q) Quantification of MMC (Lhx3^{on}, FoxP1^{off}), LMC (Raldh2^{on}, FoxP1^{high}), PGC (pSmad^{on}), and HMC (Isl1^{on}, FoxP1^{off}) MNs in E16.5 control and *mir-17∼92* $^{MN\uparrow}$ embryos (number of positive cells per 20 μm of spinal cord in the ventral half section) (mean ± SD, n = 4 embryos, **p < 0.01).

(R) Restoration of PTEN by crossing *PTEN* $^{f/+}$ with *Olig2*$^{Cre/+}$*;mir-17∼92*^{floxed} mice partially rescues the reduction of FoxP1^{on} LMC-MNs in *mir-17∼92*$^{MN\Delta}$ embryos.

(S) Quantification of LMC-MNs (FoxP1^{on}, ChAT^{on}) in the lumbar spinal cord in the control (*Olig2*$^{Cre/+}$; *PTEN* $^{f/+}$), KO (*Olig2*$^{Cre/+}$*;mir-17∼92* $^{f/f}$), and rescue (*Olig2*$^{Cre/+}$*;mir-17∼92* $^{f/f}$, *PTEN* $^{f/+}$) embryos. LMC-MNs are significantly rescued after PTEN deletion (**p < 0.01) (mean ± SD, n = 4 embryos).

occurring MN death. To test this, we overexpressed *mir-17∼92* in MNs from *Olig2*$^{Cre/+}$*; ROSA26-loxp-STOP-loxp-mir-17∼92* (*mir-17∼92*$^{MN\uparrow}$) crosses (Figure 7). Comparison of the spinal cords of mice overexpressing *mir-17∼92* to their control littermates at E12.5 revealed a drastic reduction in PTEN expression and nuclear accumulation (Figures 7A and 7B). Consequently, we observed a significant change in the number and distribution of MNs within the ventral horn of the developing spinal cord at E16.5. While LMCs and MMCs were well segregated in control brachial and lumbar spinal cords at this stage, a band of MNs connecting the two columns appeared in the animals overexpressing *mir-17∼92* (Figures 7C–7J). The ectopically positioned MNs displayed smaller nuclei (Figures 7K and 7L), consistent with *Bax*$^{-/-}$ embryos (Buss et al., 2006a). Other MN subtypes (MMC- and HMC-MNs) appeared unchanged in the *mir-17∼92*$^{MN\uparrow}$ embryos (Figures 7M–7P, quantification in Figure 7Q). These studies demonstrate that overexpression of the *mir-17∼92* cluster rescued these cells from programmed cell death.

Attenuation of PTEN Elicited by *mir-17∼92* Depletion Rescues LMC-MN Apoptosis

If *mir-17∼92* indeed targets *PTEN* and regulates its subcellular localization to control LMC-MN survival, we would expect that restoring the PTEN level could rescue the apoptosis phenotype. To test this hypothesis, we generated and analyzed *mir-17∼92*$^{MN\Delta}$ mice with *PTEN*$^{MN\Delta/+}$. The control (*Olig2*$^{Cre/+}$*; PTEN* $^{f/+}$) embryos did not manifest any obvious differences in the number of FoxP1^{on} LMC-MNs relative to their WT littermates. However, compared to the embryos from KO (*Olig2*$^{Cre/+}$*; mir-17∼92*$^{f/f}$) mice, embryos from *PTEN*-rescued mice (*Olig2*$^{Cre/+}$*; mir-17∼92*$^{f/f}$*; PTEN* $^{f/+}$) exhibited significantly higher numbers of FoxP1^{on} LMC-MNs (Figures 7R and 7S). Therefore, these results demonstrate that reducing the amount of PTEN protein back to the basal level can largely rescue the selective LMC-MN degeneration in the *mir-17∼92*$^{MN\Delta}$ mutants. Together, our results provide evidence that the inhibition of PTEN expression caused by *mir-17∼92* deletion rescues MN apoptosis, while the overexpression of *mir-17∼92* in pMNs prevents naturally occurring cell death during neural development by attenuating PTEN expression and nuclear import.

DISCUSSION

Mir-17∼92 Acts as a Double-Edged Sword that Controls MN Generation and Degeneration

Our previous study revealed that *mir-17-3p* in the *mir-17∼92* cluster is critical for carving out the boundary of pMN/p2 progenitors (Chen et al., 2011). We demonstrated that postmitotic MNs expand into the V2 interneuron domain ectopically in the spinal cord of *mir-17∼92*-null embryos at E9.5. However, conditional deletion of the miRNA processing enzyme *Dicer* from all MN progenitors (*Dicer*$^{MN\Delta}$) leads to the loss of many limb- and sympathetic-ganglia-innervating spinal MNs (Chen and Wichterle, 2012). This suggests that miRNAs play multifaceted roles during MN generation. At the progenitor stage, miRNA is critical for establishing the progenitor boundary, whereas postmitotically, miRNAs are required to maintain MN survival and subtype identity. In this study, we uncovered that the *mir-17∼92* cluster is responsible for the selective degeneration of the MN subtype. Functional characterization of the conditional *mir-17∼92*$^{MN\Delta}$ in vitro and in vivo confirmed the importance of *mir-17∼92* in sustaining MN survival, in addition to its function in Olig2 inhibition at the progenitor stage. These results indicate that the *mir-17∼92* cluster functions as a double-edged sword that controls MN generation and degeneration in the developing spinal cord. We also suggest that *mir-17∼92* is the major culprit responsible for the selective limb-innervating MN apoptosis phenotype in *Dicer*$^{MN\Delta}$ embryos. Unlike the erosion of motor pool identity and the perinatal lethality observed in *Dicer*$^{MN\Delta}$ embryos, the spared LMC-MNs of *mir-17∼92*$^{MN\Delta}$ embryos still expressed several pool markers. Future experiments are necessary to determine which miRNAs are required to establish motor pool identity.

mir-17∼92 Exhibits Intrinsic and Cell-Autonomous Functions in LMC Neurons

As MNs are the only neurons that project axons out of the CNS to innervate targets, their survival is controlled by target-derived trophic factors (Hamburger, 1992; Oppenheim, 1989; Taylor et al., 2012). In addition, GDNF and proprioceptive afferent neurons impinging on MNs also contribute to the survival surveillance of MNs (Kanning et al., 2010). Emerging evidence also demonstrates that MN degeneration in amyotrophic lateral sclerosis (ALS) can be accelerated by co-culturing MNs with diseased astrocytes in vitro (Di Giorgio et al., 2007; Dimos et al., 2008). Here, using in vitro and in vivo approaches, we tested whether LMC-MN cell death is cell autonomous and provide four lines of evidence supporting the intrinsic functions of *mir-17∼92* in maintaining LMC-MN survival: (1) the expression of *mir-17∼92* is more enriched in *FoxP1::GFP* cells in vitro and in FoxP1^{on} MNs in vivo compared to other MN subtypes; (2) "salt and pepper" mixing experiments indicate that only *mir-17∼92*$^{-/-}$ MNs are dying, while control *Hb9::RFP*^{on} MNs are unaffected; (3) LMC-MNs degenerate in conditional *mir-17∼92*$^{MN\Delta}$ embryos, which phenocopies LMC cell death in the *mir-17∼92*-null embryos; and (4) interneurons and glial cells are not affected in the conditional *mir-17∼92*$^{MN\Delta}$ embryos.

Intrinsic and Extrinsic MN Survival Control

Why, in the absence of *mir-17∼92*, do only LMC-MNs undergo selective degeneration in the spinal cord? In the developing CNS, ∼20%–85% of the differentiated cells degenerate during development (Buss et al., 2006b; Oppenheim, 1991). Several hypotheses have been suggested to explain why MNs are initially overproduced and then undergo cell death as they differentiate. One proposed "NF hypothesis" suggests that the overproduced MNs compete for a limited amount of NFs when they reach the innervating targets, implying that the purpose of the naturally occurring neuronal death is to match the number of afferent nerves with the size of the target population (Buss et al., 2006b; Dekkers et al., 2013; Oppenheim, 1989). However, this hypothesis is mainly based on peripheral nervous system studies. Emerging evidence has demonstrated fundamental differences between naturally occurring cell death in the peripheral nervous system and CNS. For example, BDNF is the most widely expressed neurotrophin in the CNS, yet the number of neurons in most CNS areas is not affected upon its deletion (Ernfors et al., 1994). Moreover, recent studies have indicated that cell-to-cell contacts and synaptic transmission control the survival of neurons in the CNS (Nikoletopoulou et al., 2010) and that the cell death of developing cortical interneurons is intrinsically determined without the interference of NFs (Dekkers and Barde, 2013; Southwell et al., 2012).

In addition, based on our observation that LMC-MNs degenerate at ∼E12.5–E13.5 in the *mir-17∼92* mutants, the time point at which LMC-MNs are just about to establish their target connections, and because the LMC-MNs could not be rescued by the addition of NF cocktails while the naturally occurring MN death is rescued in *mir-17∼92* $^{MN\Delta}$ embryos, we herein propose an alternative "intrinsic and extrinsic cross-talk model" for LMC-MNs, in which *mir-17∼92* acts as an intrinsic guardian providing protection by inhibiting apoptotic pathways prior to target contact. Once MN axons reach the muscle targets, retrograde NFs provide the nutrient source, thus generating another layer of protection for the existing MNs to support their long-term survival. LMC-MNs integrate intrinsic and extrinsic pro- and

anti-apoptotic signals to allow their axons to navigate the remarkably long journey to their final destinations. The cross-talk model might provide a more comprehensive explanation for the intricate apoptosis regulation in the developing CNS, reminiscent of the programmed cell death observed early and at later stages in chick motor neurons (Yaginuma et al., 1996). As our NF-dependent experiments were performed in vitro, future in vivo genetic manipulations of NF receptors and transplantation experiments are required to determine to what extent the *mir-17∼92*-mediated cell-autonomous apoptosis in LMC-MNs is solely intrinsic.

Specific LMC Degeneration in the Absence of *mir-17∼92*

Both the *mir-17∼92*$^{-/-}$ and conditional *mir-17∼92*$^{MN\Delta}$ embryos showed selective degeneration of the limb-innervating MNs, which is consistent with the *Dicer*$^{MN\Delta}$ embryos. This differs from a previous study indicating that an increase in apoptosis is only observed in the double KOs of *mir-17∼92* and its paralog, *miR-106b-25* (Ventura et al., 2008). We attribute this discrepancy to the different spinal cord segments examined in our study compared to those examined in the previous report. We scrutinized and performed serial analyses of mutant and control spinal cords and determined that the increases in apoptosis are spinal segment dependent. We observed increased apoptosis in the brachial and lumbar spinal cords but detected only a mild elevation in apoptosis in the thoracic segment. Moreover, limb-level MNs were significantly reduced in number, while the numbers of other MN subtypes remained similar. It is likely that the previous study examined only the thoracic region, as it is the largest segment in the spinal cord.

The *mir17∼92* Cluster and PTEN Subcellular Localization

How does *mir-17∼92* regulate MN subtype survival? Several studies have shown that *mir-17∼92* can promote proliferation, increase angiogenesis, and sustain cell survival via the post-transcriptional repression of a number of target mRNAs (Bian et al., 2013; Mu et al., 2009; Olive et al., 2010). As the pleiotropic functions of *mir-17∼92* are dependent on cell type and physiological context, we utilized unbiased approaches to systematically shed light on the MN targets. First, we identified mRNAs that are upregulated in *mir-17∼92*-null MNs in vitro and in vivo. Second, we filtered these genes with the in-silico-predicted *mir-17∼92* targets. Finally, we reasoned that, if the targets are MN context dependent, then the target expression levels would not be affected in non-MNs of *mir-17∼92*-KO embryos.

With these stringent criteria, we narrowed our examination to 15 targets. *PTEN* was our primary focus, as several reports have already revealed that the interplay between *PTEN* and *mir-17∼92* is important for regulating cell survival (Bian et al., 2013; Mu et al., 2009; Olive et al., 2010; Zhang et al., 2013b). Immunostaining and western blotting not only confirmed the increase in PTEN expression but also showed a striking nuclear accumulation of PTEN in the LMC-MNs of *mir-17∼92*-KO embryos. Early studies indicated that the Nedd4 family, together with their associated protein Ndfip1, can regulate the monoubiquitination of PTEN, as well as the import of PTEN into the nucleus (Howitt et al., 2012; Trotman et al., 2007). Surprisingly, we found that the expression of several genes associated with E3 ligases were also upregulated in *mir-17∼92*$^{-/-}$ MNs. In this study, we verified by luciferase assays that *Ndifp1*, *Nedd4-2*, and other E3 ubiquitin ligases were bona fide targets of *mir-17∼92*. Additionally, we found that overexpressing *mir-17∼92* causes the reduction of PTEN^{monoUb} and PTEN^{nucleus} in vitro, indicating that *mir-17∼92* not only targets *PTEN* directly but also regulates the subcellular localization of PTEN by targeting E3 ubiquitin ligase complexes. Recent studies have highlighted the importance of nuclear PTEN in neurons and in tumors (reviewed in Kreis et al., 2014; Song et al., 2012), yet whether nuclear PTEN functions as a pro-survival or pro-apoptotic protein in neurons remains controversial (Bassi et al., 2013; Howitt et al., 2012). Our analyses demonstrate that *mir-17∼92* mediates the level of nuclear PTEN and that the restoration of PTEN to basal levels partially rescues MN cell death in conditional *mir-17∼92*$^{MN\Delta}$ embryos, thereby emphasizing the role of nuclear PTEN in governing neuronal survival. Here, we also suggest a new mode of regulation by miRNA, one that not only mediates target expression but also controls target subcellular localization. This might also provide an explanation for why miRNAs are generally clustered in the mammalian genomes, as they may orchestrate target functions by regulating gene expression and post-translational modification in a coherent manner (He et al., 2005; Olive et al., 2010, 2013). Future dissection of the individual miRNAs responsible for target expression and subcellular localization will be interesting.

In addition to the role of nuclear PTEN in LMC-MNs uncovered in this study, PTEN has also been found to translocate into the nucleus in response to neuronal injuries such as ischemia, traumatic brain injury, and N-methyl-D-aspartate-induced excitotoxicity (Goh et al., 2014; Howitt et al., 2012; Zhang et al., 2013a). Consistent with these previous results, we also demonstrated that inhibiting the nuclear translocation of PTEN using a peptide designed to block the K13/K289-ubiquitination of PTEN exhibits neuroprotective effects (Zhang et al., 2013a), emphasizing the role of nuclear PTEN in neuronal degeneration. As nuclear PTEN accumulation appears to be LMC-MN-exclusive in *mir-17∼92*$^{MN\Delta}$ embryos and as LMC-MNs are the most vulnerable MN subtype to degenerate in patients with ALS (Kanning et al., 2010; Kaplan et al., 2014), this raises the possibility that an intrinsic MN subtype modifier, such as PTEN, might contribute to the vulnerability of limb-innervating MNs in ALS (Kaplan et al., 2014). Interestingly, it has been shown that inhibiting PTEN in the mouse model for spinal muscular atrophy (SMA) rescues MN-associated defects in axon length, increases survival, and restores growth cone size (Ning et al., 2010). Similarly, microarray analysis of superoxide dismutase 1 (SOD1) mutant ALS spinal cord MNs reveals that several components of the phosphatidylinositol 3-kinase signaling pathway, including PTEN, are dysregulated in patients with ALS (Kirby et al., 2011). Thus, the exploration of *mir-17∼92*/PTEN subcellular localization may also provide a new avenue for treating selective MN subtype vulnerabilities in ALS and SMA in the future.

EXPERIMENTAL PROCEDURES

Mouse ESC Culture and Differentiation

Hb9::GFP ESCs were cultured and differentiated into spinal MNs, as previously described (Chen et al., 2011; Wichterle et al., 2002). The *FoxP1::GFP* ESC line is a transgenic reporter line that contains a BAC with ~195 kb of the 5′ FoxP1 sequence and GFP inserted at the initiating codon (a kind gift from Jeremy Dasen and Hynek Wichterle) (Jung et al., 2014). To promote caudal LMC neuron differentiation, 100 ng/ml basic fibroblast growth factor (bFGF) was included together with reduced concentrations of retinoic acid (RA) and Smoothened agonist (SAG) at day 2 of differentiation (Mazzoni et al., 2013). Cells were trypsinized and collected for FACS at day 8 to purify *FoxP1::GFP*^{high} LMC neurons and *FoxP1::GFP*^{off} non-LMC neurons for quantitative real-time PCR analysis.

Mouse Crosses and In Vivo Studies

For the KO mouse study, the generation of the *mir-17~92*$^{-/-}$ mouse was performed as described in Ventura et al. (2008). Embryos were analyzed between E12.5 and E13.5. Conditional MN-KO mice were generated by crossing *Olig2*$^{Cre/+}$ mice (Chen and Wichterle, 2012) with *mir-17~92*$^{loxp/loxp}$ mice (Ventura et al., 2008) to generate the *Olig2*$^{Cre/+}$*; mir-17~92*$^{loxp/WT}$ strain. *Olig2*$^{Cre/+}$*; mir-17~92*$^{loxp/WT}$ mice were then mated with *mir-17~92*$^{loxp/loxp}$ mice for experimental analysis. Embryos were analyzed between E11.5 and E16.5. The *Olig2*$^{Cre/+}$*; mir-17~92*$^{loxp/loxp}$ mice were further mated with *PTEN*$^{loxp/loxp}$ mice (Groszer et al., 2001) to perform target gene rescue experiments.

For the overexpression study, *Olig2*$^{Cre/+}$ mice (Dessaud et al., 2007) were mated with *ROSA26* $^{CAG\text{-}MIR17\text{-}92,\text{-}EGFP}$ mice (Xiao et al., 2008) to generate the *Olig2*$^{Cre/+}$*; ROSA26* $^{CAG\text{-}MIR17\text{-}92,\text{-}EGFP}$ strain. Embryos were analyzed at ~E15.5–16.5.

Quantitative Real-Time PCR

ESCs or EBs were harvested for total RNA isolation using the mirVana kit (Ambion). For mRNA analysis, 20 ng of total RNA from each sample was reverse transcribed with Superscript III (Invitrogen). One-tenth of the reverse transcription reaction was used for subsequent quantitative real-time PCRs, which were performed in duplicate per sample, with at least three independent experimental samples, on the LightCycler480 Real Time PCR instrument (Roche) using SYBR Green PCR mix (Roche) for each gene of interest and glyceraldehyde 3-phosphate dehydrogenase controls for normalization.

For the miRNA analysis, 5 ng of total RNA was reverse transcribed with a miRNA-specific primer from TaqMan MicroRNA Assays (Life Technology). A ubiquitous small nucleolar RNA, sno234, was used as the endogenous control. Each quantitative real-time PCR was performed in duplicate or triplicate per sample, with at least three different experimental samples.

Immunostaining and Immunoblotting Antibodies

For the list of antibodies, please refer to the Supplemental Experimental Procedures. Images were collected on a Zeiss LSM710 Meta Confocal Microscope.

miRNA In Situ Hybridization with Immunostaining

In situ hybridizations were performed as described previously (Chen et al., 2007, 2011) and in Supplemental Experimental Procedures.

ACCESSION NUMBERS

All microarray data reported in this paper have been deposited to the NCBI GEO and are available under accession number GEO:GSE67795.

SUPPLEMENTAL INFORMATION

Supplemental Information includes Supplemental Experimental Procedures, five figures, five tables, and one movie and can be found with this article online at http://dx.doi.org/10.1016/j.celrep.2015.04.050.

AUTHOR CONTRIBUTIONS

Y.-T.T. and Y.-L.L. designed and conceived the study. K.-C.P. performed the luciferase analysis. Y.-P.Y. and M.C. helped to maintain and analyze mouse experiments. J.L. and J.-H.H. performed and analyzed microarray data. S.T. generated *Hb9::RFP* ESC lines and Y.-P.H. and H.J. generated *FoxP1::GFP* mouse line and ESC. J.-A.C. interpreted the data and wrote the manuscript.

ACKNOWLEDGMENTS

We thank the Microarray Core in IMB for performing the microarray experiments in addition to Ya-Min Lin in the FACS core facility, Sue-Ping Lee in the imaging core facility, and Paul Hsu in the Bioinformatics Core at IMB for their strong technical help. We thank T. Jessell (Columbia University) and S. Morton for the antibody gifts and J. Dasen (NYU) for providing the *FoxP1::GFP* transgenic mouse. We also acknowledge H. Wichterle and S. Nedelec for their insightful and critical comments on the manuscript, A.J. Giraldez and F.C. Tang for discussing the experimental results, and the IMB Scientific English Editing Core for further reviewing the manuscript. J.-A.C. is supported by Academia Sinica and an NSC fellowship, and Y.-T.T. is supported by a National Science Council Fellowship (102-2811-B-001 −073). Y.-P.H. was supported by NIH NICD grant R21 NS076936. This work is funded by Academia Sinica, NSC (101-2314-B-001 −004 -MY3 and 102-2321-B-001 −057), and NHRI (NHRI-EX103-10315NC).

Received: November 19, 2014
Revised: March 17, 2015
Accepted: April 22, 2015
Published: May 21, 2015

REFERENCES

Asli, N.S., and Kessel, M. (2010). Spatiotemporally restricted regulation of generic motor neuron programs by miR-196-mediated repression of Hoxb8. Dev. Biol. *344*, 857–868.

Bassi, C., Ho, J., Srikumar, T., Dowling, R.J., Gorrini, C., Miller, S.J., Mak, T.W., Neel, B.G., Raught, B., and Stambolic, V. (2013). Nuclear PTEN controls DNA repair and sensitivity to genotoxic stress. Science *341*, 395–399.

Bian, S., Hong, J., Li, Q., Schebelle, L., Pollock, A., Knauss, J.L., Garg, V., and Sun, T. (2013). MicroRNA cluster miR-17-92 regulates neural stem cell expansion and transition to intermediate progenitors in the developing mouse neocortex. Cell Rep. *3*, 1398–1406.

Burek, M.J., and Oppenheim, R.W. (1996). Programmed cell death in the developing nervous system. Brain Pathol. *6*, 427–446.

Buss, R.R., Gould, T.W., Ma, J., Vinsant, S., Prevette, D., Winseck, A., Toops, K.A., Hammarback, J.A., Smith, T.L., and Oppenheim, R.W. (2006a). Neuromuscular development in the absence of programmed cell death: phenotypic alteration of motoneurons and muscle. J. Neurosci. *26*, 13413–13427.

Buss, R.R., Sun, W., and Oppenheim, R.W. (2006b). Adaptive roles of programmed cell death during nervous system development. Annu. Rev. Neurosci. *29*, 1–35.

Chen, J.A., and Wichterle, H. (2012). Apoptosis of limb innervating motor neurons and erosion of motor pool identity upon lineage specific dicer inactivation. Front Neurosci *6*, 69.

Chen, J.A., Chu, S.T., and Amaya, E. (2007). Maintenance of motor neuron progenitors in Xenopus requires a novel localized cyclin. EMBO Rep. *8*, 287–292.

Chen, J.A., Huang, Y.P., Mazzoni, E.O., Tan, G.C., Zavadil, J., and Wichterle, H. (2011). Mir-17-3p controls spinal neural progenitor patterning by regulating Olig2/Irx3 cross-repressive loop. Neuron *69*, 721–735.

Dalla Torre di Sanguinetto, S.A., Dasen, J.S., and Arber, S. (2008). Transcriptional mechanisms controlling motor neuron diversity and connectivity. Curr. Opin. Neurobiol. *18*, 36–43.

Dasen, J.S. (2009). Transcriptional networks in the early development of sensory-motor circuits. Curr. Top. Dev. Biol. *87*, 119–148.

Dasen, J.S., and Jessell, T.M. (2009). Hox networks and the origins of motor neuron diversity. Curr. Top. Dev. Biol. *88*, 169–200.

Dasen, J.S., Tice, B.C., Brenner-Morton, S., and Jessell, T.M. (2005). A Hox regulatory network establishes motor neuron pool identity and target-muscle connectivity. Cell *123*, 477–491.

Dasen, J.S., De Camilli, A., Wang, B., Tucker, P.W., and Jessell, T.M. (2008). Hox repertoires for motor neuron diversity and connectivity gated by a single accessory factor, FoxP1. Cell *134*, 304–316.

Dekkers, M.P., and Barde, Y.A. (2013). Developmental biology. Programmed cell death in neuronal development. Science *340*, 39–41.

Dekkers, M.P., Nikoletopoulou, V., and Barde, Y.A. (2013). Cell biology in neuroscience: Death of developing neurons: new insights and implications for connectivity. J. Cell Biol. *203*, 385–393.

Dessaud, E., Yang, L.L., Hill, K., Cox, B., Ulloa, F., Ribeiro, A., Mynett, A., Novitch, B.G., and Briscoe, J. (2007). Interpretation of the sonic hedgehog morphogen gradient by a temporal adaptation mechanism. Nature *450*, 717–720.

Dessaud, E., McMahon, A.P., and Briscoe, J. (2008). Pattern formation in the vertebrate neural tube: a sonic hedgehog morphogen-regulated transcriptional network. Development *135*, 2489–2503.

Di Giorgio, F.P., Carrasco, M.A., Siao, M.C., Maniatis, T., and Eggan, K. (2007). Non-cell autonomous effect of glia on motor neurons in an embryonic stem cell-based ALS model. Nat. Neurosci. *10*, 608–614.

Dimos, J.T., Rodolfa, K.T., Niakan, K.K., Weisenthal, L.M., Mitsumoto, H., Chung, W., Croft, G.F., Saphier, G., Leibel, R., Goland, R., et al. (2008). Induced pluripotent stem cells generated from patients with ALS can be differentiated into motor neurons. Science *321*, 1218–1221.

Ernfors, P., Lee, K.F., and Jaenisch, R. (1994). Mice lacking brain-derived neurotrophic factor develop with sensory deficits. Nature *368*, 147–150.

Goh, C.P., Putz, U., Howitt, J., Low, L.H., Gunnersen, J., Bye, N., Morganti-Kossmann, C., and Tan, S.S. (2014). Nuclear trafficking of Pten after brain injury leads to neuron survival not death. Exp. Neurol. *252*, 37–46.

Grimson, A., Farh, K.K., Johnston, W.K., Garrett-Engele, P., Lim, L.P., and Bartel, D.P. (2007). MicroRNA targeting specificity in mammals: determinants beyond seed pairing. Mol. Cell *27*, 91–105.

Groszer, M., Erickson, R., Scripture-Adams, D.D., Lesche, R., Trumpp, A., Zack, J.A., Kornblum, H.I., Liu, X., and Wu, H. (2001). Negative regulation of neural stem/progenitor cell proliferation by the Pten tumor suppressor gene in vivo. Science *294*, 2186–2189.

Hamburger, V. (1992). History of the discovery of neuronal death in embryos. J. Neurobiol. *23*, 1116–1123.

He, L., Thomson, J.M., Hemann, M.T., Hernando-Monge, E., Mu, D., Goodson, S., Powers, S., Cordon-Cardo, C., Lowe, S.W., Hannon, G.J., and Hammond, S.M. (2005). A microRNA polycistron as a potential human oncogene. Nature *435*, 828–833.

Howitt, J., Lackovic, J., Low, L.H., Naguib, A., Macintyre, A., Goh, C.P., Callaway, J.K., Hammond, V., Thomas, T., Dixon, M., et al. (2012). Ndfip1 regulates nuclear Pten import in vivo to promote neuronal survival following cerebral ischemia. J. Cell Biol. *196*, 29–36.

Huang, W., Sherman, B.T., and Lempicki, R.A. (2009). Systematic and integrative analysis of large gene lists using DAVID bioinformatics resources. Nat. Protoc. *4*, 44–57.

Jung, H., Mazzoni, E.O., Soshnikova, N., Hanley, O., Venkatesh, B., Duboule, D., and Dasen, J.S. (2014). Evolving Hox activity profiles govern diversity in locomotor systems. Dev. Cell *29*, 171–187.

Kanning, K.C., Kaplan, A., and Henderson, C.E. (2010). Motor neuron diversity in development and disease. Annu. Rev. Neurosci. *33*, 409–440.

Kaplan, A., Spiller, K.J., Towne, C., Kanning, K.C., Choe, G.T., Geber, A., Akay, T., Aebischer, P., and Henderson, C.E. (2014). Neuronal matrix metalloproteinase-9 is a determinant of selective neurodegeneration. Neuron *81*, 333–348.

Kreis, P., Leondaritis, G., Lieberam, I., and Eickholt, B.J. (2014). Subcellular targeting and dynamic regulation of PTEN: implications for neuronal cells and neurological disorders. Front. Mol. Neurosci. *7*, 23.

Mazzoni, E.O., Mahony, S., Peljto, M., Patel, T., Thornton, S.R., McCuine, S., Reeder, C., Boyer, L.A., Young, R.A., Gifford, D.K., and Wichterle, H. (2013). Saltatory remodeling of Hox chromatin in response to rostrocaudal patterning signals. Nat. Neurosci. *16*, 1191–1198.

Mu, P., Han, Y.C., Betel, D., Yao, E., Squatrito, M., Ogrodowski, P., de Stanchina, E., D'Andrea, A., Sander, C., and Ventura, A. (2009). Genetic dissection of the miR-17~92 cluster of microRNAs in Myc-induced B-cell lymphomas. Genes Dev. *23*, 2806–2811.

Mund, T., and Pelham, H.R. (2010). Regulation of PTEN/Akt and MAP kinase signaling pathways by the ubiquitin ligase activators Ndfip1 and Ndfip2. Proc. Natl. Acad. Sci. USA *107*, 11429–11434.

Nikoletopoulou, V., Lickert, H., Frade, J.M., Rencurel, C., Giallonardo, P., Zhang, L., Bibel, M., and Barde, Y.A. (2010). Neurotrophin receptors TrkA and TrkC cause neuronal death whereas TrkB does not. Nature *467*, 59–63.

Ning, K., Drepper, C., Valori, C.F., Ahsan, M., Wyles, M., Higginbottom, A., Herrmann, T., Shaw, P., Azzouz, M., and Sendtner, M. (2010). PTEN depletion rescues axonal growth defect and improves survival in SMN-deficient motor neurons. Hum. Mol. Genet. *19*, 3159–3168.

Olive, V., Bennett, M.J., Walker, J.C., Ma, C., Jiang, I., Cordon-Cardo, C., Li, Q.J., Lowe, S.W., Hannon, G.J., and He, L. (2009). miR-19 is a key oncogenic component of mir-17-92. Genes Dev. *23*, 2839–2849.

Olive, V., Jiang, I., and He, L. (2010). mir-17-92, a cluster of miRNAs in the midst of the cancer network. Int. J. Biochem. Cell Biol. *42*, 1348–1354.

Olive, V., Sabio, E., Bennett, M.J., De Jong, C.S., Biton, A., McGann, J.C., Greaney, S.K., Sodir, N.M., Zhou, A.Y., Balakrishnan, A., et al. (2013). A component of the mir-17-92 polycistronic oncomir promotes oncogene-dependent apoptosis. eLife *2*, e00822.

Oppenheim, R.W. (1989). The neurotrophic theory and naturally occurring motoneuron death. Trends Neurosci. *12*, 252–255.

Oppenheim, R.W. (1991). Cell death during development of the nervous system. Annu. Rev. Neurosci. *14*, 453–501.

Otaegi, G., Pollock, A., Hong, J., and Sun, T. (2011). MicroRNA miR-9 modifies motor neuron columns by a tuning regulation of FoxP1 levels in developing spinal cords. J. Neurosci. *31*, 809–818.

Philippidou, P., and Dasen, J.S. (2013). Hox genes: choreographers in neural development, architects of circuit organization. Neuron *80*, 12–34.

Raff, M.C. (1992). Social controls on cell survival and cell death. Nature *356*, 397–400.

Raoul, C., Henderson, C.E., and Pettmann, B. (1999). Programmed cell death of embryonic motoneurons triggered through the Fas death receptor. J. Cell Biol. *147*, 1049–1062.

Rousso, D.L., Gaber, Z.B., Wellik, D., Morrisey, E.E., and Novitch, B.G. (2008). Coordinated actions of the forkhead protein Foxp1 and Hox proteins in the columnar organization of spinal motor neurons. Neuron *59*, 226–240.

Song, M.S., Carracedo, A., Salmena, L., Song, S.J., Egia, A., Malumbres, M., and Pandolfi, P.P. (2011). Nuclear PTEN regulates the APC-CDH1 tumor-suppressive complex in a phosphatase-independent manner. Cell *144*, 187–199.

Song, M.S., Salmena, L., and Pandolfi, P.P. (2012). The functions and regulation of the PTEN tumour suppressor. Nat. Rev. Mol. Cell Biol. *13*, 283–296.

Southwell, D.G., Paredes, M.F., Galvao, R.P., Jones, D.L., Froemke, R.C., Sebe, J.Y., Alfaro-Cervello, C., Tang, Y., Garcia-Verdugo, J.M., Rubenstein, J.L., et al. (2012). Intrinsically determined cell death of developing cortical interneurons. Nature *491*, 109–113.

Taylor, A.R., Gifondorwa, D.J., Robinson, M.B., Strupe, J.L., Prevette, D., Johnson, J.E., Hempstead, B., Oppenheim, R.W., and Milligan, C.E. (2012). Motoneuron programmed cell death in response to proBDNF. Dev. Neurobiol. *72*, 699–712.

Trotman, L.C., Wang, X., Alimonti, A., Chen, Z., Teruya-Feldstein, J., Yang, H., Pavletich, N.P., Carver, B.S., Cordon-Cardo, C., Erdjument-Bromage, H., et al.

(2007). Ubiquitination regulates PTEN nuclear import and tumor suppression. Cell *128*, 141–156.

Van Themsche, C., Leblanc, V., Parent, S., and Asselin, E. (2009). X-linked inhibitor of apoptosis protein (XIAP) regulates PTEN ubiquitination, content, and compartmentalization. J. Biol. Chem. *284*, 20462–20466.

Ventura, A., Young, A.G., Winslow, M.M., Lintault, L., Meissner, A., Erkeland, S.J., Newman, J., Bronson, R.T., Crowley, D., Stone, J.R., et al. (2008). Targeted deletion reveals essential and overlapping functions of the miR-17 through 92 family of miRNA clusters. Cell *132*, 875–886.

Wichterle, H., Lieberam, I., Porter, J.A., and Jessell, T.M. (2002). Directed differentiation of embryonic stem cells into motor neurons. Cell *110*, 385–397.

Xiao, C., Srinivasan, L., Calado, D.P., Patterson, H.C., Zhang, B., Wang, J., Henderson, J.M., Kutok, J.L., and Rajewsky, K. (2008). Lymphoproliferative disease and autoimmunity in mice with increased miR-17-92 expression in lymphocytes. Nat. Immunol. *9*, 405–414.

Yaginuma, H., Tomita, M., Takashita, N., McKay, S.E., Cardwell, C., Yin, Q.W., and Oppenheim, R.W. (1996). A novel type of programmed neuronal death in the cervical spinal cord of the chick embryo. J. Neurosci. *16*, 3685–3703.

Zhang, S., Taghibiglou, C., Girling, K., Dong, Z., Lin, S.Z., Lee, W., Shyu, W.C., and Wang, Y.T. (2013a). Critical role of increased PTEN nuclear translocation in excitotoxic and ischemic neuronal injuries. J. Neurosci. *33*, 7997–8008.

Zhang, Y., Ueno, Y., Liu, X.S., Buller, B., Wang, X., Chopp, M., and Zhang, Z.G. (2013b). The MicroRNA-17-92 cluster enhances axonal outgrowth in embryonic cortical neurons. J. Neurosci. *33*, 6885–6894.

Kirby, J., Ning, K., Ferraiuolo, L., Heath, P.R., Ismail, A., Kuo, S.W., Valori, C.F., Cox, L., Sharrack, B., Wharton, S.B., et al. (2011). Phosphatase and tensin homologue/protein kinase B pathway linked to motor neuron survival in human superoxide dismutase 1-related amyotrophic lateral sclerosis. Brain *134*, 506–517.